Received: 4 January 2024 | Accepted: 9 May 2024

DOI: 10.1002/jmv.29684

RESEARCH ARTICLE

JOURNAL OF MEDICAL VIROLOGY WILEY

# Unveiling the role of KSHV-infected human mesenchymal stem cells in Kaposi's sarcoma initiation

Ezequiel Lacunza[1,2] | Anuj Ahuja[3,4] | Omar A. Coso[2,5] | Martin Abba[1,2] | Juan Carlos Ramos[2,6,7,8] | Ethel Cesarman[4] | Enrique A. Mesri[2,3,†] | Julian Naipauer[2,5]

[1]Centro de Investigaciones Inmunologicas Basicas y Aplicadas, Facultad de Ciencias Medicas, Universidad Nacional de La Plata, La Plata, Argentina

[2]University of Miami-Centre for AIDS Research/Sylvester Cancer Comprehensive Center Argentina Consortium for Research and Training in Virally Induced AIDS-Malignancies, University of Miami Miller School of Medicine, Miami, Florida, USA

[3]Tumor Biology Program, Sylvester Comprehensive Cancer Center and Miami Center for AIDS Research, Department of Microbiology and Immunology, University of Miami Miller School of Medicine, Miami, Florida, USA

[4]Department of Pathology and Laboratory Medicine, Weill Cornell Medicine, New York, New York, USA

[5]Instituto de Fisiología, Biología Molecular y Neurociencias (IFIBYNE), CONICET-Universidad de Buenos Aires, Buenos Aires, Argentina

[6]Department of Medicine, Division of Hematology, Sylvester Comprehensive Cancer Center, University of Miami Miller School of Medicine, Miami, Florida, USA

[7]Center for AIDS Research, University of Miami Miller School of Medicine, Miami, Florida, USA

[8]Department of Microbiology and Immunology, University of Miami Miller School of Medicine, Miami, Florida, USA

**Correspondence**

Julian Naipauer, University of Miami-Centre for AIDS Research/Sylvester Cancer Comprehensive Center Argentina Consortium for Research and Training in Virally Induced AIDS-Malignancies, University of Miami Miller School of Medicine, Miami, FL, USA; Instituto de Fisiología, Biología Molecular y Neurociencias (IFIBYNE), CONICET-Universidad de Buenos Aires, Buenos Aires, Argentina.
Email: juliannaipauer@gmail.com

**Funding information**

National Cancer Institute; Miami CFAR Pilot, Grant/Award Number: P30AI073961; National Institutes of Health (NIH), Grant/Award Number: U54CA221208; National Cancer Institute of the National Institutes of Health, Grant/Award Number: P30CA240139; NIH, Grant/Award Number: CA136387

## Abstract

Kaposi's sarcoma (KS) may derive from Kaposi's sarcoma herpesvirus (KSHV)-infected human mesenchymal stem cells (hMSCs) that migrate to sites characterized by inflammation and angiogenesis, promoting the initiation of KS. By analyzing the RNA sequences of KSHV-infected primary hMSCs, we have identified specific cell subpopulations, mechanisms, and conditions involved in the initial stages of KSHV-induced transformation and reprogramming of hMSCs into KS progenitor cells. Under proangiogenic environmental conditions, KSHV can reprogram hMSCs to exhibit gene expression profiles more similar to KS tumors, activating cell cycle progression, cytokine signaling pathways, endothelial differentiation, and upregulating KSHV oncogenes indicating the involvement of KSHV infection in inducing the mesenchymal-to-endothelial (MEndT) transition of hMSCs. This finding underscores the significance of this condition in facilitating KSHV-induced proliferation and reprogramming of hMSCs towards MEndT and closer to KS gene expression profiles, providing further evidence of these cell subpopulations as precursors of KS cells that thrive in a proangiogenic environment.

Ezequiel Lacunza and Anuj Ahuja contributed equally to this study.

[†]Died August 27, 2022.

KEYWORDS
Kaposi's sarcoma, KSHV, mesenchymal-to-endothelial transition

## 1 | INTRODUCTION

Kaposi's sarcoma (KS) is an angioproliferative disease caused by the human herpesvirus 8 (HHV-8) or Kaposi's sarcoma herpesvirus (KSHV).[1] Cytokine production and angiogenesis have been shown to contribute to KS pathogenesis.[2] High levels of IL-6, TNF-α, and IL-10 were identified in sera of KS patients,[3] and KS tumors have shown elevated levels of IL-6, IL-10, and IFN-γ.[4] The identification of the precursor cell for KS is still under debate because the spindle cells found in KS lesions express different markers, which define endothelial, mesenchymal, and macrophage features.[5] KS models made from mouse endothelial lineage derived from bone marrow and KSHV-infected primary rat embryonic metanephric circulating mesenchymal precursor cells showed KS-like tumor formation in nude mice, indicating the transformation capacity of KSHV in these cellular types.[6,7] Although these are not human cells, numerous viral and cellular genes and their related pathways have subsequently been identified using these models. To shed light on the process of KSHV-induced tumorigenesis and transformation, research has focused on human mesenchymal stem cells (MSC). Notably, KSHV infection of human MSC (hMSC) has been demonstrated to result in an increased expression of a wide range of chemokines, cytokines, and their receptors.[8–11]

Furthermore, KSHV infection of oral mesenchymal stem cells induces mesenchymal-to-endothelial transition (MEndT) and leads to the increased expression of angiogenic factors.[9] Clinical research on Kaposi sarcoma specimens has provided supporting evidence for MEndT in the disease, as KS samples show positive markers for CD105 (Endoglin), CD34, COX-2, VEGF, α-SMA, and c-Kit.[12] A study by Wang et al. has recently shown that KSHV infection of periodontal ligament stem cells (PDLSCs) significantly upregulates the expression of chemokine receptors and promotes the migration and settlement of MSCs at wound sites.[13] Similarly, Chen et al. demonstrated that KSHV infection of MSCs initiates an incomplete MEndT process, generating hybrid mesenchymal/endothelial (M/E) state cells, which are abundant in KS lesions.[14]

Interestingly, KSHV infection of human MSCs exhibits different outcomes depending on their culture conditions. Under basal MSC culture conditions, viral production is favored, but infected cell proliferation is impaired. In contrast, KS-like proangiogenic culture conditions support the proliferation of productively infected hMSC cultures. Moreover, only KS-like proangiogenic conditions induce tumorigenesis in PDGFRA-positive mouse bone marrow-derived MSCs infected with KSHV.[15] These findings support the hypothesis that KS may arise from KSHV-infected MSCs that migrate to inflammatory and proangiogenic sites, thereby enhancing the transformation and reprogramming capacity of KSHV. However, several aspects related to the cell progenitor subpopulation, defining markers, underlying mechanisms, and specific conditions governing KSHV-induced transformation and reprogramming of MSCs into KS-precursors remain incompletely understood. Further research is needed to fully elucidate these aspects.[16]

In this study, we conducted KSHV infection experiments on primary bone marrow-derived human MSCs, comparing two different environmental conditions: basal and proangiogenic scenarios. Subsequently, we performed whole RNA-sequencing and pathway analysis on the differentially expressed genes (DEGs) at two time points: 72 h postinfection to examine short-term reprogramming effects induced by KSHV, and 1 month after the selection of infected cells to uncover long-term changes. Our analysis revealed that human MSCs infected in proangiogenic environments exhibited significant overrepresentation and activation of pathways related to cytokine activity, cell proliferation, and angiogenesis. This indicates the crucial role of proangiogenic conditions in the KSHV-induced reprogramming of hMSCs. Protein extracts were subjected to analysis using cytokine and angiogenesis arrays, confirming the upregulation of relevant factors in KS-like conditions. These findings support the boosting effect of KS-like proangiogenic conditions in reprogramming hMSCs towards MEndT by KSHV infection. Moreover, the analysis of genes directly influenced by KSHV infection in proangiogenic conditions revealed significant associations with endothelial differentiation, cytokine signaling pathways, and cell cycle progression. This finding further highlights the role of KSHV infection in inducing MEndT and promoting proliferation in KSHV-infected hMSCs.

Our results demonstrate the importance of the KS-like proangiogenic growth environment in the KSHV-induced reprogramming of hMSCs towards endothelial differentiation and proliferation. This reinforces the notion that this subpopulation of infected cells growing in a proangiogenic environment could potentially serve as KS precursors.

## 2 | RESULTS

### 2.1 | RNA-sequencing analysis of de novo infected bone marrow-derived hMSC in different cell culture conditions

To evaluate the impact of different growth conditions in KSHV infection of bone marrow-derived human mesenchymal stem cells (hMSC), we infected these cells with KSHV in different environments. We performed KSHV (KSHVr.219)[17] infection of hMSC in MEM alpha medium, basal MSC growth conditions (MSC-KSHV$^{MEM}$), or KS-like proangiogenic conditions (MSC-KSHV$^{KS}$). The cellular mechanisms that promote inflammation, wound repair, and angiogenesis may play a relevant role in the development of Kaposi sarcoma tumors in individuals infected with KSHV (KS-like proangiogenic environment). To recreate this KS-like proangiogenic environment in vitro, we cultured hMSCs after infection in a cell culture media enriched with heparin, BME vitamin, endothelial cell growth supplement (ECGS), and

endothelial cell growth factors (ECGF). This approach reproduced a proangiogenic/vasculogenic environment in the cell culture media.[18,19] After 72 h of infection (short-term infection) or after 1 month of infection and selection for KSHV-infected cells (long-term infection), we extracted RNA to perform a whole RNA-sequencing analysis. As controls for both time points, we included mock-infected hMSCs growing under basal MSC growth conditions ($MSC^{MEM}$) and mock-infected hMSCs growing in KS-like proangiogenic conditions ($MSC^{KS}$) to study the effects of the proangiogenic environment (Figure 1A,B). The multidimensional scaling plot demonstrated noticeable changes in the hMSC transcriptome due to KSHV infection and the KS-like growth conditions (Figure 1C,D). At short-term infection, the biggest changes are produced by the KS-like proangiogenic environment and KSHV infection (Figure 1C). After long-term infection and selection, the transcriptomic differences between uninfected cells are small, but between KSHV-infected cells, these differences remain large and even increase due to long-term KSHV infection (Figure 1D). These results provide important insights into how KSHV infection and the proangiogenic environment can influence the gene expression patterns of hMSCs, potentially contributing to Kaposi Sarcoma development. We used an IncuCyte® Live-Cell Imaging and Analysis System to follow the infection and amount of green fluorescent protein (GFP)-positive populations of KSHV-infected hMSCs growing in MSC or KS-like media, and, as previously observed,[15] GFP-positive population (KSHV-infected cells) of MSC-$KSHV^{KS}$ continues to increase over time while the GFP-positive population (KSHV-infected cells) of KSHV-$MSC^{MEM}$ stopped increasing shortly after KSHV infection (Figure 1E). After 72 h of infection in both environments, we observed GFP-positive and red fluorescent protein (RFP)-positive cells (Figure 1F), indicating latent and lytic infection of hMSC after KSHV infection.

## 2.2 | KSHV infection in KS-like proangiogenic environmental conditions reprograms human MSCs to increase cytokine, cell proliferation, and angiogenic markers

We compared the gene expression profiles of uninfected cells with their respective infected counterparts to better understand the impact of KSHV infection in the two environments (Table S1). Subsequently, we conducted pathways analysis of these DEGs (Table S2). Using Gene Ontology (GO), we observed significant activation of regulation of innate immune response at short-term infection in both environmental conditions and regulation of defense response, and cytokine-mediated signaling only in KS-like conditions at both time points (Figure 2A,C and Table S2). Using the hallmark of cancer, we observed activation of hallmark interferon alpha response, hallmark interferon-gamma response, and hallmark inflammatory response in both environmental conditions at short-term infection. Interestingly, these same pathways (hallmark interferon alpha response, and hallmark interferon-gamma response) remain activated only in KS-like proangiogenic conditions at long-term infection (Figure 2B,D and Table S2).

To validate these RNA-sequencing findings, we conducted cytokine and angiogenesis arrays on protein extracts from MSC-$KSHV^{MEM}$ and MSC-$KSHV^{KS}$ cells after 72 h (short-term infection) of infection or after 1 month of infection and selection for KSHV-infected cells (long-term infection), examining over one hundred different cytokines and fifty angiogenesis-related proteins (Figure 3). Among the differentially regulated cytokines, we observed CXCL8/iL8, CCL2, Pentraxin 3, and Chitinase 3-like 1 as the top significantly upregulated cytokines in KSHV-infected hMSC growing in a KS-like environment (Figure 3A). In the angiogenic array, we found upregulation of uPA, Serpine E1 (PAI1), Serpine F1, Endoglin, Pentraxin 3, and CXCL8/iL8 as the top significantly upregulated factors in the KSHV-infected hMSC growing in a KS-like environment (Figure 3B). In contrast, we found FGFb, FGFa, DPPIV, Coagulation Factor III, and VEGF significantly upregulated in KSHV-hMSC growing in basal conditions (Figure 3A,B). These findings strongly support the notion that KS-like conditions boost the reprogramming of hMSCs by KSHV infection towards angiogenesis and cytokine pathways. The observed activation of these pathways sheds light on the potential mechanisms by which KSHV-infected hMSCs contribute to angiogenesis and inflammation responses, which may play critical roles in the development of Kaposi's sarcoma. To further characterize these cells, we performed a western blot analysis of mesenchymal and endothelial markers. Moreover, we also added Cyclin D1 and phosphor-AKT as markers of proliferation (Figure 3C). This new data shows that KSHV-infected hMSC growing in a KS-like environment express higher levels of Cyclin D1 and phospho-AKT, along with upregulation of mesenchymal (PDGFRA) and endothelial (CD31/PECAM-1) markers.

## 2.3 | KSHV infection in a proangiogenic environment activates the proliferation of hMSCs with progenitor cell markers

To compare the effects of KSHV infection in hMSCs under basal MSC growth conditions and KS-like proangiogenic conditions at different time points after infection, we analyzed the DEGs between the two infected cell types, namely MSC-$KSHV^{MEM}$ versus MSC-$KSHV^{KS}$ (Table S3). Subsequently, we conducted pathways analysis of these DEGs (Table S4). We identified the cell cycle as the most prominently activated pathway using GO in hMSCs infected in the KS-like proangiogenic environment at both time points (Figure 4A,D and Table S4), correlated with the increase in proliferation of these infected cells (Figure 1E). The heatmap in Figure S1 illustrates the DEGs associated with the mitotic nuclear division pathway implicated in the cell cycle (Figure S1). Using Hallmark, we found activation of hallmark interferon alpha response, hallmark interferon-gamma response, and hallmark inflammatory response, as observed in Figure 2 (Figure 4B,E and Table S4).

Additionally, the long-term selection of KSHV-infected hMSCs growing in a KS-like proangiogenic environment showed activation of hypoxia, a significant hallmark of Kaposi's sarcoma tumors (Figure 4E

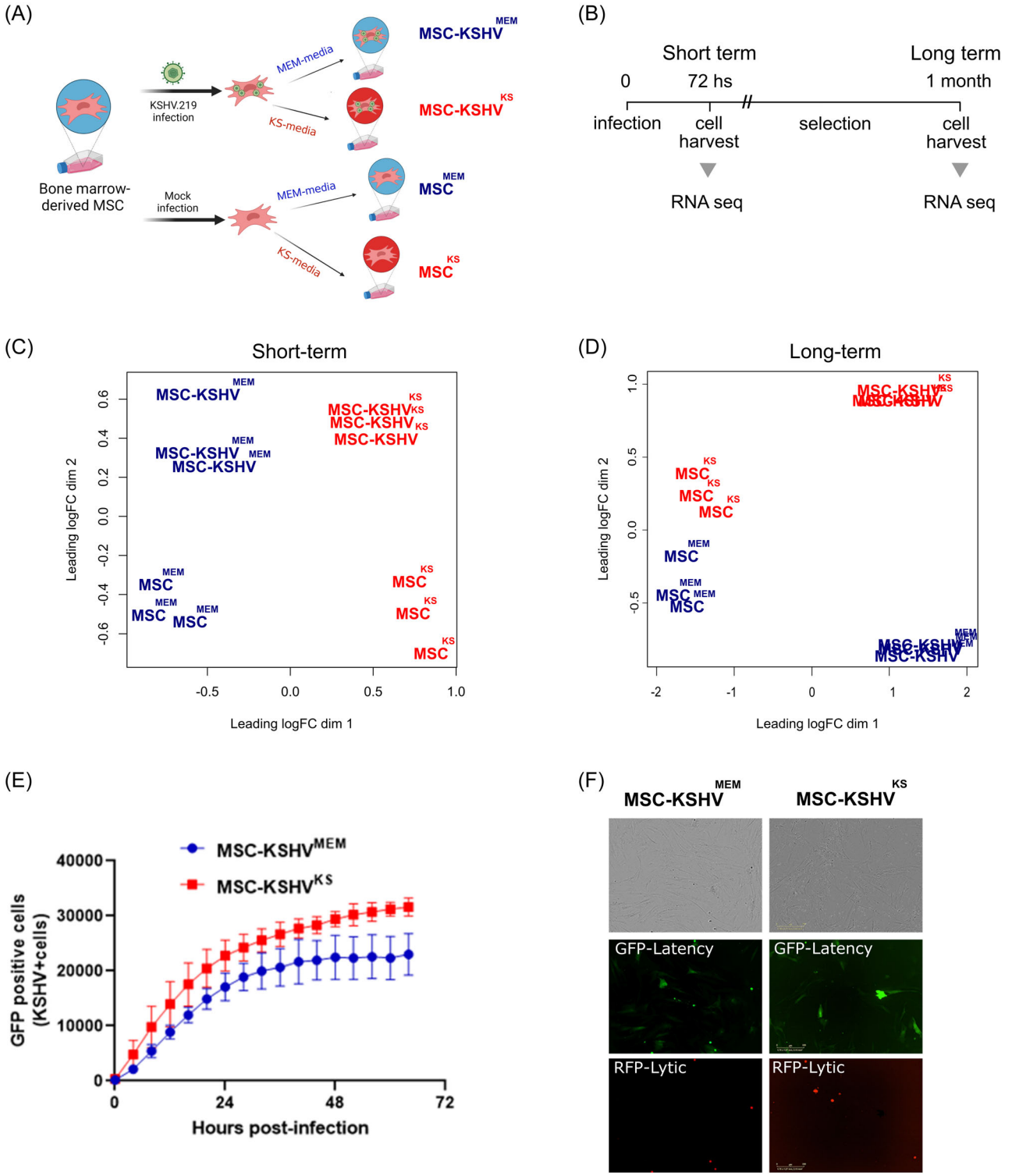


**FIGURE 1** RNA-sequencing analysis of de novo infected bone marrow-derived hMSC in different environments. (A) Schematic representation of the experimental design and samples group assignment. (B) Sequenced samples and times after infection: 72 h after infection (short-term infection) or 1 month after infection and selection (long-term infection). (C) Multidimensional scaling plot of the host RNA at short-term infection showing the distance of each sample from each other determined by their leading log fold change. (D) Multidimensional scaling plot of the host RNA at long-term infection and selection for infected cells showing the distance of each sample from each other determined by their leading log fold change. (E) hMSCs were infected with KSHV in MSC or KS-like media and incubated in an Incucyte Zoom (Essen Bioscience), acquiring green fluorescence images. The amount of latently infected cells (GFP-positive) is plotted over time. The graph shows the mean ± standard error from three replicates for each condition. (F) Fluorescence microscopy images were acquired from the Incucyte Zoom, using the GFP reporter driven by the constitutive promoter of cellular EF-1 and the RFP reporter driven by the early lytic gene PAN promoter at 72 h postinfection. GFP, green fluorescent protein; hMSC, human mesenchymal stem cells; KSHV, Kaposi's sarcoma herpesvirus; PAN, polyadenylated nuclear RNA; RFP, red fluorescent protein.

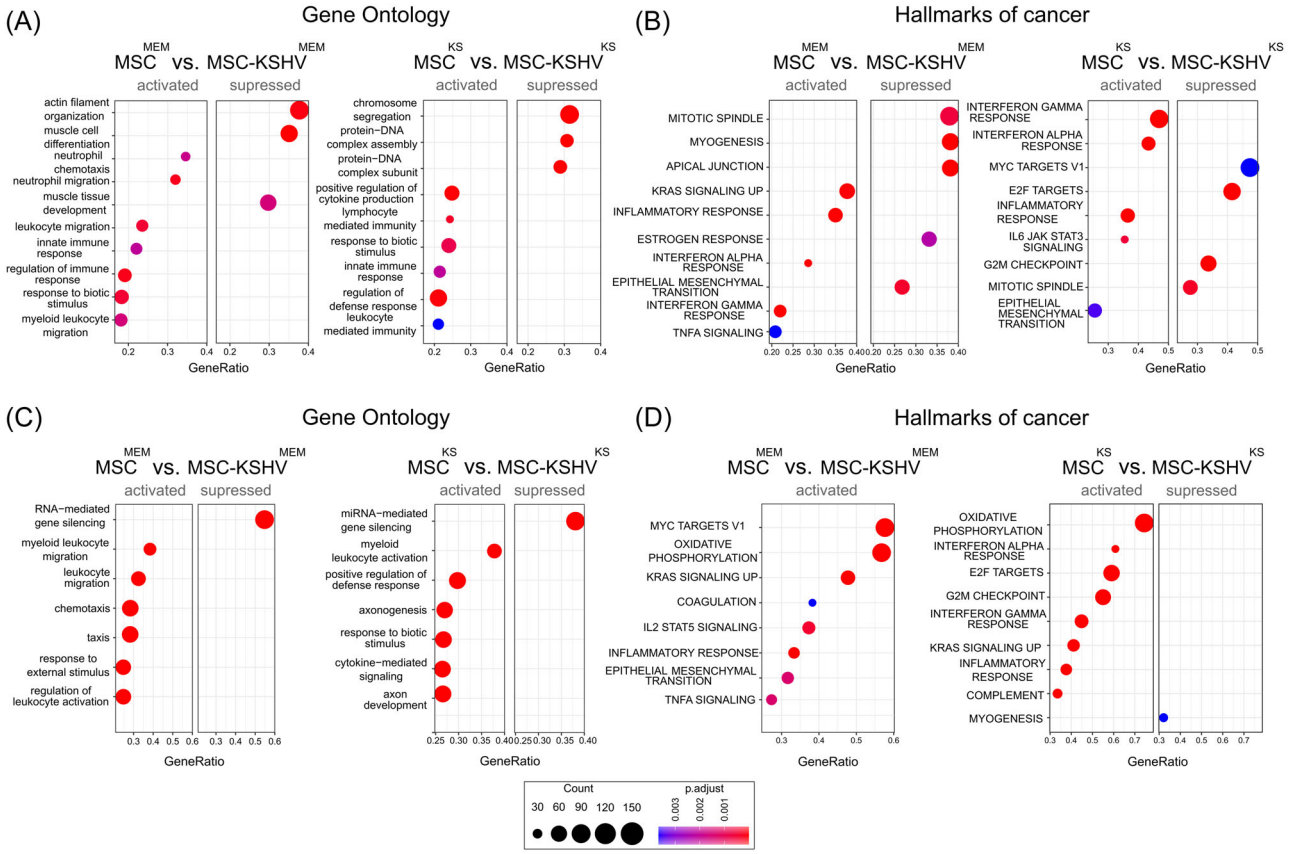


**FIGURE 2** Differential gene expression analysis and functional enrichment of transcriptomic data. Dot plots of gene set enrichment analysis obtained from the comparisons between control and infected cells in both environmental conditions at short- and long-term infection. (A) Dot plot of significantly activated and suppressed Gene Ontology pathways in infected cells after 72 h of infection in both MEM and KS environment. (B) Dot plot of significantly activated and suppressed Hallmarks of Cancer in infected cells after 72hs of infection in both MEM and KS environment. (C) Dot plot of significantly activated and suppressed Gene Ontology pathways in infected cells after long-term infection and selection in both MEM and KS environments. (D) Dot plot of significantly activated and suppressed Hallmarks of Cancer in infected cells after long-term infection and selection in both MEM and KS environments. Each dot represents a specific biological term, with the size of the dot indicating the number of genes associated with that term. The color of the dots corresponds to the adjusted *p* value, highlighting the significance of enrichment. KS, Kaposi's sarcoma; MEM, minimum essential medium.

and Table S4). Furthermore, using Cell marker only KSHV-infected hMSCs cultured in the KS-like proangiogenic environment at both time points exhibited an enrichment of MkI67+ progenitor cells, which are stem-like genes markers of proliferation, as well as endothelial cells (Figure 4C,F and Table S4). These findings indicate that KSHV infection in KS-like proangiogenic conditions reprograms hMSCs through a mesenchymal-to-endothelial transition and induces the proliferation of these progenitor cells.

## 2.4 | KSHV infection drives endothelial differentiation, cell cycle progression, and chemokine signaling of hMSC in the KS-like environment

To understand whether the observed changes in host gene expression shown in Figures 1–4 are induced by KSHV, the proangiogenic environment, or a combination of both factors, we conducted an analysis of DEGs between hMSCs cultured in basal MSC or KS-like conditions in the presence or absence of KSHV. Results revealed 258 genes that were directly influenced by KSHV infection in the KS-like proangiogenic conditions at short-term infection (Figure 5A). Pathway analysis of these DEGs identified Endothelial Differentiation as the most significant upregulated pathway (Figure 5C and Table S5). Several genes involved in this pathway, including ROBO4, IKBKB, XDH, and WNT7B, were most upregulated in MSC-KSHV$^{KS}$ cells. Suggesting that these genes might play a critical role in the initial steps of the KSHV-induced reprogramming of hMSCs towards a mesenchymal-to-endothelial transition within the proangiogenic environment. Remarkably, at long-term infection and selection for infected cells, the number of DEGs directly dependent on KSHV infection in the KS-like media increased to 1305, indicating a more profound effect of a KSHV-induced reprogramming after long-term selection for infected cells in KS-like proangiogenic conditions (Figure 5B). We found the chemokine-mediated signaling pathway and mitotic cell cycle phase transition among

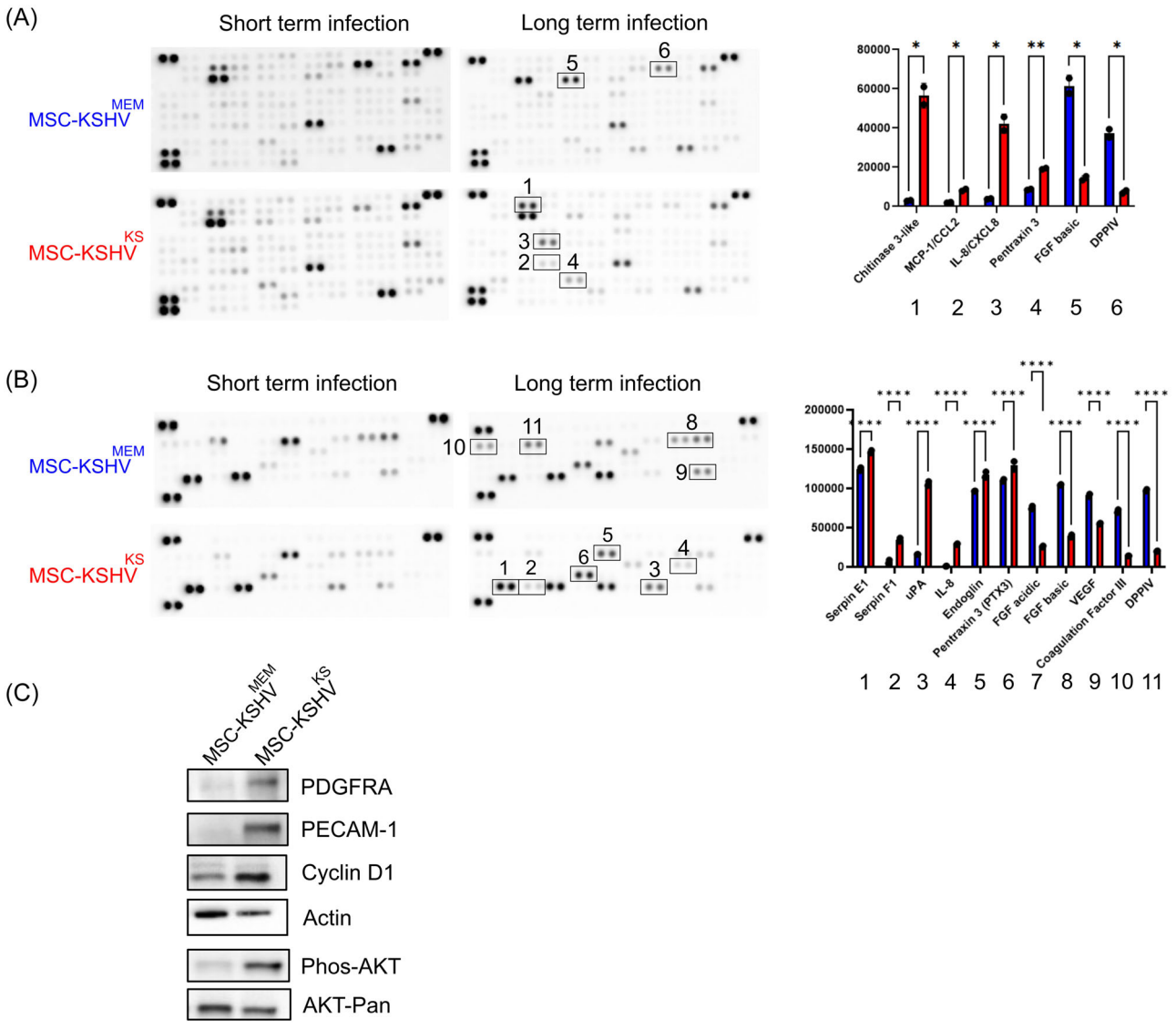


**FIGURE 3** Cytokine and angiogenesis arrays to validate the RNA-sequencing findings. (A) Cytokine Array Kit was used to quantify levels of 105 cytokines in MSC-KSHV$^{MEM}$ and MSC-KSHV$^{KS}$ at short-term infection and long-term infection and selection for infected cells pointing to major activation spots corresponding to the statistically upregulated cytokines. (B) Angiogenesis Array Kit was used to quantify levels of 55 angiogenesis-related proteins in MSC-KSHV$^{MEM}$ and MSC-KSHV$^{KS}$ at short-term infection or long-term infection and selection for infected cells pointing to major activation spots corresponding to the statistically upregulated proteins. (C) PDGFRA (mesenchymal marker), CD31/PECAM-1 (endothelial marker), phospho-AKT, AKT, and Cyclin D1 protein levels in hMSC after 72 h of KSHV infection. Actin was used as the loading control. hMSC, human mesenchymal stem cells; KS, Kaposi's sarcoma; KSHV, Kaposi's sarcoma herpesvirus; MEM, minimum essential medium; MSC, mesenchymal stem cell.

the enriched pathways in KSHV-infected hMSCs growing in a KS-like environment after selection for infected cells (Figure 5D and Table S5). Among the DEGs related to chemokines, we found CXCL1/Gro-alpha and CXCL2/Gro-beta, both cytokines, involved in KS tumorigenesis, suggesting their potential role in the disease progression. Related to the cell cycle we found CCNA2, CCND2, CCNB2, CDC20, CDC25A, and CDC25C as DEGs specifically regulated by KSHV in KS-like proangiogenic environment after selection for infected cells.

## 2.5 | Genome-wide analysis of KSHV transcriptome showed an increase in KSHV gene expression in a proangiogenic environment

To evaluate the differences in KSHV gene expression in hMSC subjected to different environmental conditions and times after infection, we performed a genome-wide analysis of the whole KSHV transcriptome comparing KSHV gene expression between MSC-KSHV$^{MEM}$ and MSC-KSHV$^{KS}$ at short-term infection or long-term

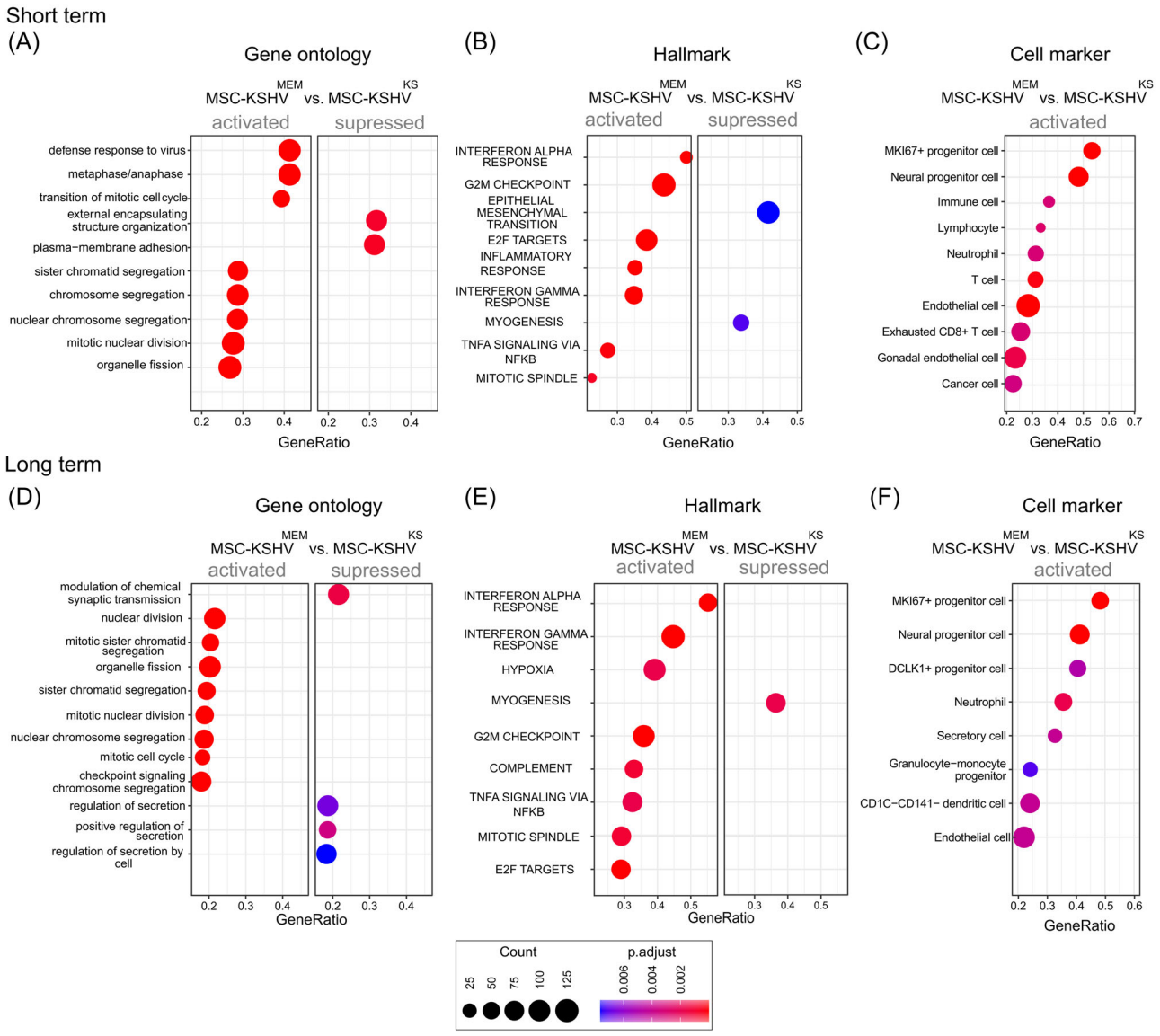


**FIGURE 4** Gene set enrichment analysis (GSEA) of differentially expressed genes (DEG) in the comparison between MSC-KSHV$^{MEM}$ and MSC-KSHV$^{KS}$ cells at short-term and long-term infection. (A)–(C) Dot plots of significantly activated and suppressed Gene Ontology (GO) pathways (A), Hallmark (B), and Cell Marker (C) in MSC-KSHV$^{KS}$ cells after 72 h of infection. (D)–(F) Significantly enriched activated and suppressed GO (D), Cell Marker (E), and Hallmark (F) between the two infected cell types at long-term infection. Each dot represents a specific biological term, with the size of the dot indicating the number of genes associated with that term. The color of the dots corresponds to the adjusted *p* value, highlighting the significance of enrichment. KS, Kaposi's sarcoma; KSHV, Kaposi's sarcoma herpesvirus; MEM, minimum essential medium; MSC, mesenchymal stem cell.

infection and selection for infected cells. The heatmap in Figure S2 showed the expression of all KSHV genes in these samples (Figure S2). The multidimensional scaling (MDS) plot showed that MSC-KSHV$^{MEM}$ and MSC-KSHV$^{KS}$ cluster together at short-term infection, in contrast, the differences between hMSC infected in basal conditions and KS-like proangiogenic environment were more profound after long-term infection (Figure 6A). Our analysis identified 10 KSHV genes that were statistically differentially expressed between these two cell types at short-term infection, as illustrated in the volcano plot (Figure 6B and Table S6). Interestingly, after long-term selection, we identified 24 KSHV genes statistically differentially expressed between MSC-KSHV$^{MEM}$ and MSC-KSHV$^{KS}$ (Figure 6C, Table S6). ORF K2 (vIL6), ORF K12 (Kaposin), ORF 73 (LANA), ORF 71 (vFLIP), and ORF 72 (vCyclin) were the most upregulated genes in KSHV-infected hMSC growing in a KS-like proangiogenic environment upon selection (Figure 6D). Importantly, there was no significant difference in the amount of intracellular KSHV copy numbers between these KSHV-infected hMSCs (Figure S3). These viral genes would be important for the regulation of the cell cycle progression, chemokine, and hypoxia-related genes upregulated in KSHV-infected hMSC growing in a KS-like environment.

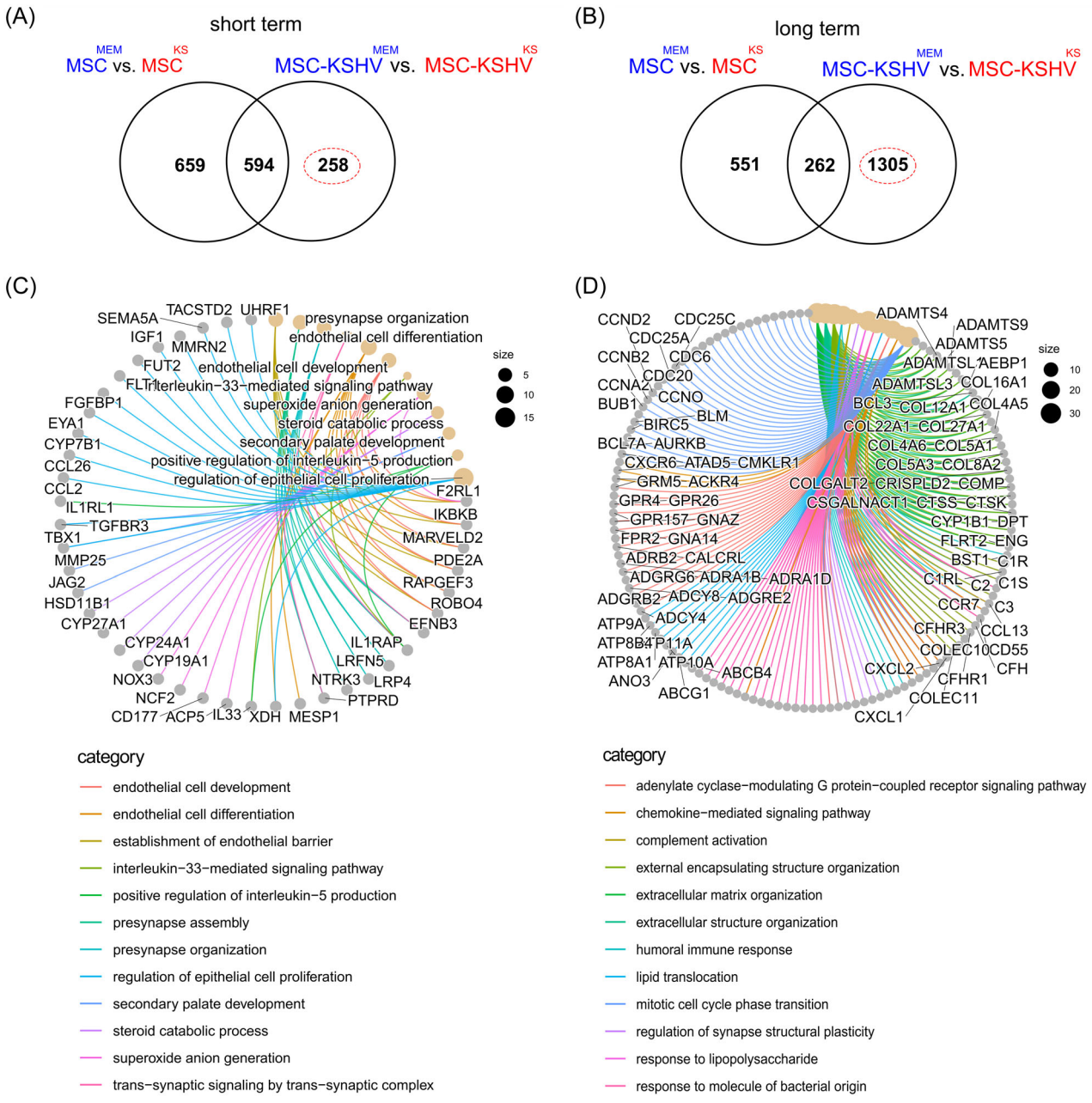


**FIGURE 5** Endothelial differentiation cell cycle progression and chemokine signaling of hMSC in the KS environment is driven by KSHV infection. (A) and (B) Schematic representation of the comparisons and DEGs found short-term infection or long-term infection and selection for infected cells. (C) and (D) Network analysis of the genes that are directly dependent on KSHV infection in KS-like proangiogenic conditions for each time point. DEGs, differentially expressed genes; hMSC, human mesenchymal stem cell; KS, Kaposi's sarcoma; KSHV, Kaposi's sarcoma herpesvirus.

## 2.6 | KSHV infection in KS proangiogenic environmental conditions reprograms human MSCs in KS-like gene expression profile

The results presented here suggest that KSHV infection in a KS-like proangiogenic environment drives the reprogramming of hMSCs, contributing to the mesenchymal-to-endothelial transition, the proliferation of progenitor cells, and the activation of hypoxia-related pathways, all of which are hallmarks of KS tumorigenesis. To gain further insights into how KSHV-infected hMSCs respond to different environments and their correlation with gene expression profiles of KS lesions, we conducted an analysis using KS signatures from the literature. Specifically, we employed a KS signature of 3589 significant DEGs between KS lesions and control samples as Tso et al. proposed.[20] Figure 7A shows unsupervised clustering of gene expression profiles using the TSO signature on hMSC samples from

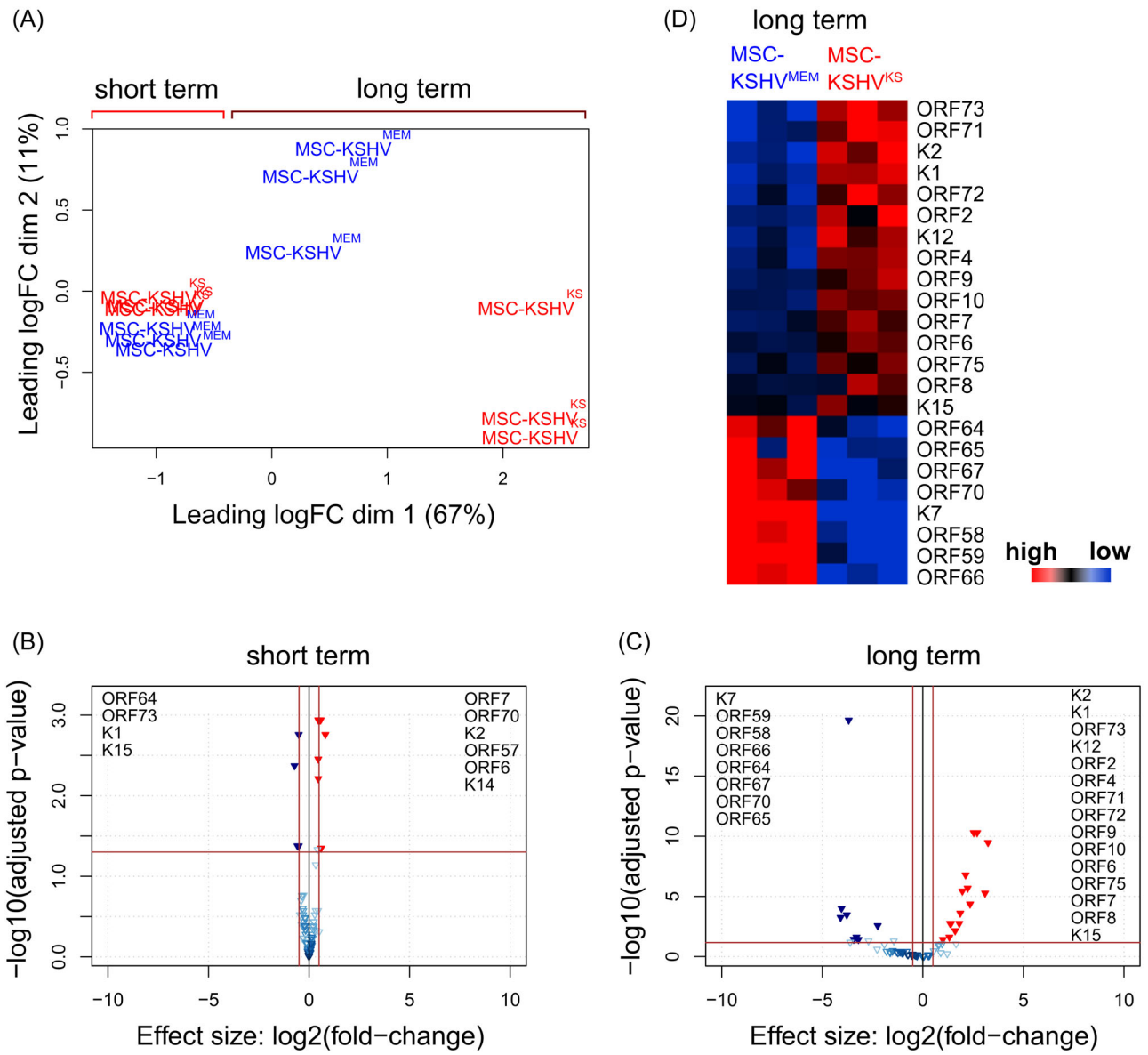


**FIGURE 6** Genome-wide analysis of KSHV transcriptome. (A) Multidimensional scaling plot of the viral RNA at short-term infection and long-term infection and selection for infected cells showing the distance of each sample from each other determined by their leading log fold change. (B) Volcano plot showing KSHV differentially expressed genes (DEGs) analyzed by RNA-sequencing between MSC-KSHV$^{MEM}$ and MSC-KSHV$^{KS}$ at short-term infection. (C) Volcano plot showing KSHV DEGs analyzed by RNA-sequencing between MSC-KSHV$^{MEM}$ and MSC-KSHV$^{KS}$ at long-term infection and selection for infected cells. (D) Heatmap of the differently expressed KSHV genes between MSC-KSHV$^{MEM}$ and MSC-KSHV$^{KS}$ at long-term infection and selection for infected cells. KS, Kaposi's sarcoma; KSHV, Kaposi's sarcoma herpesvirus; MEM, minimum essential medium; MSC, mesenchymal stem cell.

our study in the different environments and time points with and without infection, along with samples from 24 KS lesions (epidemic and endemic KS), contralateral/ipsilateral controls, and normal skin from the Lidenge study.[21] All uninfected cells, except the uninfected cells growing short-term in a KS-like environment, clustered with the control tissues and normal skin, together with the short-term infected cells growing in MSC basal conditions (Cluster 1). All the KSHV-infected cells growing in a KS-like environment clustered with KS tumors, also long-term infected cells in MSC basal conditions clustered within this group (Cluster 2). These findings suggest that the KS-like proangiogenic conditions, combined with KSHV infection, reprogram hMSCs to exhibit gene expression profiles more similar to those seen in KS lesions, indicating these cells may serve as potential KS precursors infected and growing in a proangiogenic environment.

We then analyzed KSHV gene expression profiles in the same samples. We found that KSHV gene expression can be divided into two major clusters, KSHV Gene Cluster 1 enriched in KSHV genes related to Lytic replication, structural proteins, and viral replication; and KSHV Gene Cluster 2 enriched in KSHV genes related to Latency and Immunomodulation (Figure 7B). KS tumors split into two

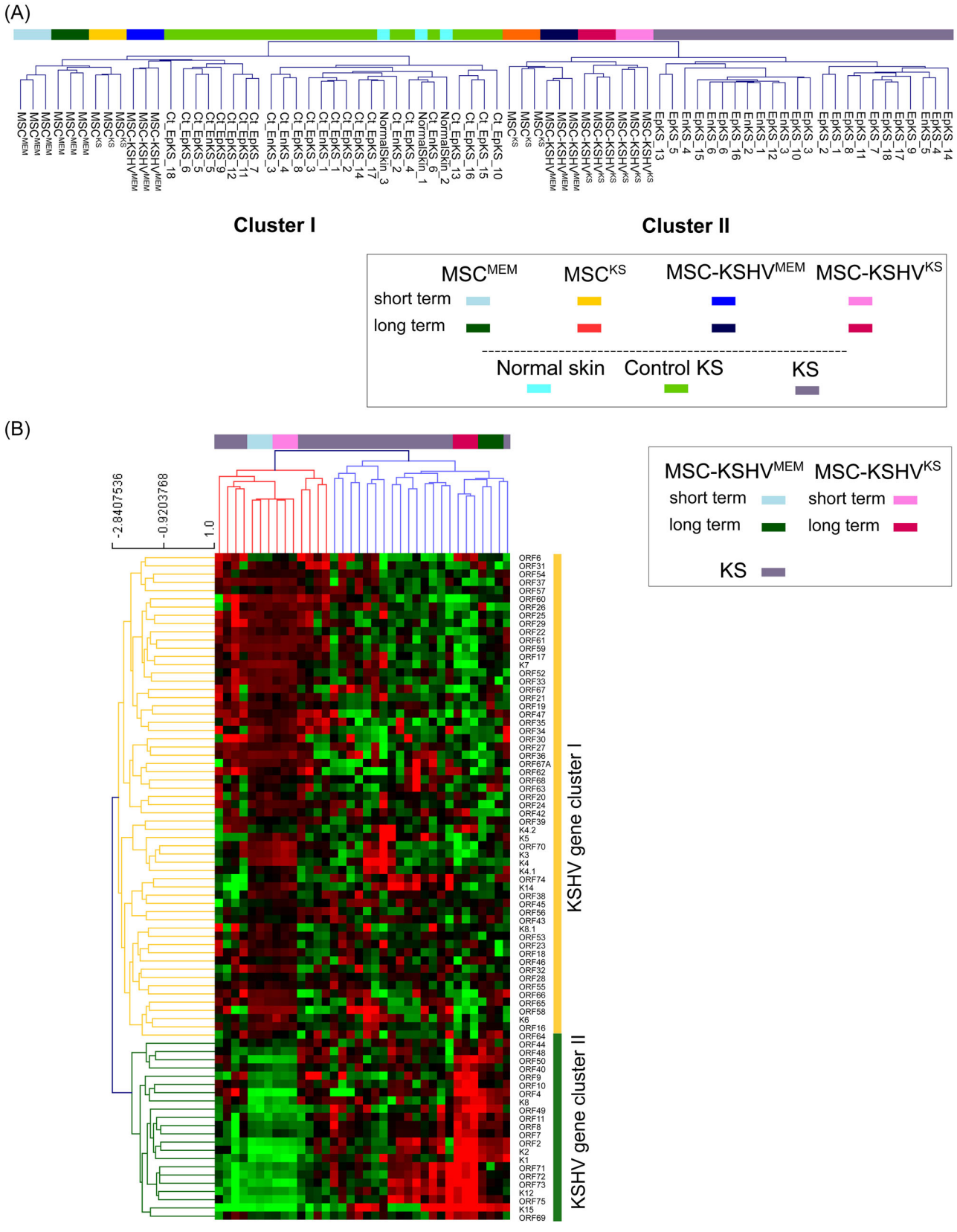


**FIGURE 7** (See caption on next page).

subgroups with different patterns of KSHV gene expression, all endemic KS and half of the epidemic KS samples clustered together with the KSHV-infected hMSC at long-term infection in both environments showing upregulation of KSHV Gene Cluster 2. The rest of the Epidemic KS samples clustered with KSHV-infected hMSC at short-term infection in both environments showing upregulation of KSHV genes in KSHV Gene Cluster 1.

## 3 | DISCUSSION

Kaposi's sarcoma remains potentially life-threatening for patients with advanced or antiretroviral therapy-resistant disease, where systemic therapy is indicated and three Food and Drug Administration-approved agents, including liposomal anthracyclines, are available.[22–24] Despite the effectiveness of these agents, most patients progress and require additional therapy.[25] Great efforts have been made to identify the KS progenitor primary cell type and the environmental conditions leading to sarcomagenesis. An emerging picture of the origin of the KS progenitor cell points to the endothelial-to-mesenchymal transition axis as important in explaining the origin of KS.[16] A better understanding of these processes would allow the development of more accurate and physiologically relevant KS models. Here, we found that processes such as angiogenesis, cell differentiation, cytokine activity, hypoxia, and cell proliferation, were significantly more overrepresented in Human mesenchymal stem cells infected with KSHV and grown in the KS-like proangiogenic environment together with increased secretion of inflammatory cytokines. We used a KS gene signature to show that KSHV infection in this environment reprograms human MSCs in a closer KS-like gene expression profile than infection in MSC cell culture conditions. Infected cells in a KS-like proangiogenic environment showed upregulation of oncogenic viral and host genes, further demonstrating the need for this environment for oncogenic viral gene expression, virus-induced reprogramming towards mesenchymal-to-endothelial transition axis and KS progenitor cell transformation initiation.

To reproduce proangiogenic KS-like culture conditions we added to the cell culture media crude preparations of endothelial cell growth factors (ECGF) with heparin, which was shown to potentiate the mitogenic activity of ECGF.[26] The main active component of these crude extracts of ECGF is basic fibroblast growth factor (bFGF), which is highly expressed at the RNA and protein level in cultured AIDS-KS cells and in spindle cells from AIDS-KS and classic KS tissue.[27,28] The whole RNA-sequencing analysis of hMSC infected in two different environments showed that KSHV infection and proangiogenic KS-like conditions significantly impact the hMSC transcriptome, directed by KSHV gene expression and the plasticity of hMSC growing in an environment rich in angiogenic factors (Figures 1 and 2). This plasticity allowed KSHV to reprogram hMSC to upregulate the expression and secretion of inflammatory cytokines like Endoglin (CD105), CXCL8/iL8, CCL2, Pentraxin 3 (PTX3), Serpin E1/PAI-1, Serpine F1, Chitinase 3-like 1, and uPA (Figure 3). Importantly, it was shown that cytokines have an important role in KS pathogenesis.[9,29–32] Moreover, KSHV infection in KS-like proangiogenic conditions reprograms hMSCs through a mesenchymal-to-endothelial transition and induces the proliferation of these progenitor cells (Figures 1E, 3, and 4).

After short-term KSHV infection in proangiogenic conditions of hMSC, KSHV specifically induced high levels of ROBO4, XDH, NOX5, and ESM1 implicated in Angiogenesis and endothelial lineage differentiation. Long-term KSHV infection of hMSC in a proangiogenic environment induces activation of chemokine–mediated signaling and mitotic cell cycle phase transition pathways suggesting their potential role in the disease progression. These results support the reprogramming effect of KSHV to induce mesenchymal-to-endothelial transition in MSCs and the boosting effect of the KS-like environment (Figure 5).

We have previously shown that de novo KSHV infection of hMSC leads to a latent and lytic infection and showed that lytic reactivation differs depending on the environmental conditions in which hMSCs are infected. With more virus production and lytic reactivation in hMSCs infected in MSC basal conditions compared with KS-like conditions. Importantly, we previously showed that hMSC infection is mostly latent with only 20% of lytic reactivation, and real-time quantitative reverse transcription polymerase chain reaction (qRT-PCR) showed no differences in KSHV LANA, RTA, and K8.1 gene expression.[15] Whole RNA-sequencing of the KSHV gene expression showed that after long-term infection and selection in a proangiogenic environment, KSHV oncogenes are upregulated and possibly involved in the reprogramming of hMSC (Figure 6).

Using a KS gene signature of 1482 genes, Li et al. found that KSHV-infected oral MSC clusters closer to KS lesions than KSHV-infected endothelial cells HMVECs, LECs, and BECs.[9] We used a KS signature of 3589 genes[20] and RNA-sequencing of 24 KS samples[21] to show that hMSC infected with KSHV in proangiogenic conditions recapitulates better the gene expression profile of KS lesions (Figure 7A). This highlights the importance of this condition in KSHV reprogramming of

**FIGURE 7** KSHV infection in KS proangiogenic environmental conditions reprograms human MSCs in KS-like gene expression profile. (A) Unsupervised clustering—resulting from the gene expression profile of a KS signature of 3589 significantly DEGs between KS lesions and control samples—on the samples from our study, together with 24 samples of KS lesions, 24 contralateral/ipsilateral controls, and three normal skin derived from the Lidenge study21. Cluster I and Cluster II are shown. (B) Unsupervised clustering—resulting from the KSHV gene expression profile—on the samples from our study and 24 samples of KS lesions from the Lidenge study21. Two main clusters of samples (red and blue) and genes (yellow and green) are identified. KSHV Gene Cluster 1 enriched in KSHV genes related to lytic replication, structural proteins, and viral replication; and KSHV Gene Cluster 2 enriched in KSHV genes related to Latency and Immunomodulation. The different samples are color-coded to improve interpretation. DEGs, differentially expressed genes; KS, Kaposi's sarcoma; KSHV, Kaposi's sarcoma herpesvirus; MSC, mesenchymal stem cell.

hMSC towards endothelial differentiation and transformation and closer to KS expression profiles, reinforcing the importance of these cells and conditions for KSHV-induced transformation. Importantly, our KSHV gene expression analysis showed two types of KS lesions that displayed different patterns of KSHV genes, one enriched in Lytic and replication viral proteins more similar to short-term KSHV infection of hMSC (half of the Epidemic KS analyzed) and the other KS lesions type enriched in Latent and immunomodulator viral proteins more similar to long-term KSHV infection of hMSC (all endemic KS and half of the epidemic KS analyzed) (Figure 7B).

We have not seen signs of cellular transformation of human MSC after KSHV infection, albeit we did observe an increase in proliferation of KSHV-infected hMSC growing in KS-like conditions. Although mouse and rat models of KS[6,7,15,33] have shown the transformation capacity of KSHV, the cellular transformation of human MSC remains challenging. Importantly, a big difference between the MSC-derived mouse and rat models with the infection of human MSC is that KSHV is only able to produce infective viral particles in human cells, inducing cell death after full lytic induction. During the last few years, evidence emerging from different experimental models of de novo KSHV-infected progenitors allowed the development of a new picture of the origin of the KS-spindle cell.[16] KS progenitor cells can be either from the endothelial or mesenchymal lineage suggesting that both cell types are probably critical for the KSHV-induced oncogenic process through the interaction between these cellular types. Identifying the KS progenitor primary environmental circuit could allow the development of more accurate models to test new-targeted therapies not only for AIDS-KS but also for different pathogenic outcomes of other virally mediated oncogenic diseases.

Chen et al. recently found that KSHV can promote an intermediate state of mesenchymal-to-endothelial differentiation of subpopulations of periodontal ligament stem cells (PDLSCs), correlated with the existence of KSHV-positive spindle cells in Kaposi sarcoma lesions displaying a mesenchymal/endothelial phenotype.[14] In this line, our sequencing transcriptomic analysis showed the existence of subpopulations of KSHV-infected hMSC growing in a KS-like proangiogenic environment expressing oncogenic viral genes and oncogenic host genes together with endothelial and mesenchymal differentiation markers, pointing to a role of these cells in KS initiation and progression through the mesenchymal-to-endothelial differentiation axis.

## 4 | MATERIALS AND METHODS

### 4.1 | Cell culture

Human MSCs were isolated as described previously.[34] Briefly, BM aspirates (25–50 mL) were purchased from AllCells under appropriate informed consent and institutional review board approval. The experiments were performed in triplicates using MSCs in Passage 3 from the same donor. All human MSC were cultured in MEM alpha media: supplemented with 20% heat-inactivated fetal bovine serum (FBS) (MSC media); or KS-like proangiogenic growth medium (KS media): Dulbecco's modified eagle medium supplemented with 30% FBS (Gemini Bioproducts), 0.2 mg/mL endothelial cell growth factor (ECGF) (Sigma-Aldrich) or (ReliaTech), 0.2 mg/mL endothelial cell growth supplement (ECGS) (Sigma-Aldrich), 1.2 mg/mL heparin (Sigma-Aldrich), insulin/transferrin/selenium (Invitrogen), 1% penicillin-streptomycin (Invitrogen), and BME vitamin (VWR Scientific).

### 4.2 | Virus preparation and infection

iSLK-219 cells harboring recombinant KSHV 219 from Don Ganem and Myoung[35] were used for virus preparation. Briefly, infectious viruses of the 219 strain were induced from the respective iSLK cells by treatment with doxycycline and sodium butyrate for 4 days. The culture supernatants were filtered through a 0.45-µm filter and centrifuged at 25 000 rpm for 2 h. The pellet was resuspended in phosphate-buffered saline (PBS) and aliquot and stored at −70°C as infectious KSHV preparations. Virus infection was performed according to the method used in a previous study, with minor modifications. Human MSCs were seeded $6 \times 10^4$ cells per well in six-well culture plates. After a day of culture, the culture medium was removed, and cells were washed with PBS. The prepared KSHV inoculum, multiplicity of infection (MOI) of 8, and 8 µg/mL of Polybrene were mixed and added to the cultured cells. After centrifugation at 700×*g* for 60 min, the inoculum was removed after 3 h, and 2 mL of culture medium was added to each well. For long-term infection and selection, cells were maintained under puromycin selection for 1 month until all the culture cells were GFP-positive.

### 4.3 | Cell proliferation assay (IncuCyte)

Cells were plated in six-well plates at 60 000 cells/well in three replicates. Cells were incubated in an Incucyte Zoom (Essen Bioscience), acquiring green images at 10× every 2 h. The Incucyte Zoom software was used to analyze and plot the results.

### 4.4 | Whole RNA-Sequencing analysis

A total of 60 000 hMSCs/well were plated in six-well plates. In addition, 24 h later hMSCs were infected with rKSHV219[17] and cultured in two different environments, MEM or KS-like proangiogenic culture conditions. Moreover, 72 h after KSHV infection (short-term infection) or 1 month after puromycin selection for infected cells (long-term infection), RNA from hMSC was isolated and purified using the RNeasy mini kit (Qiagen). RNA concentration and integrity were measured on an Agilent 2100 Bioanalyzer (Agilent Technologies). Only RNA samples with RNA integrity values (RIN) over 8.0 were considered for subsequent analysis. We performed paired-end sequencing using a NovaSeq platform. The short-read sequences were mapped to the human reference genome (GRCm38.82) by the

splice junction aligner TopHat V2.1.0. We employed several R/Bioconductor packages to accurately calculate the gene expression abundance at the whole-genome level using the aligned records (BAM files) and to identify DEGs between cell lines and tumors. The number of reads mapped to each gene is based on the TxDb. Human gene ensembles were counted, reported, and annotated using the Rsamtools, GenomicFeatures, and GenomicAlignments packages. To identify DEGs between cells, we utilized the DESeq. 2 test based on the normalized number of counts mapped to each gene. Data integration and visualization of differentially expressed transcripts were done with R/Bioconductor. KSHV transcriptome was analyzed using previous resources and the KSHV 2.0 reference genome,[36] while the edgeR test was employed for differential gene expression analysis of KSHV transcripts. For heatmaps visualization, we employed Multi Experimental Viewer Software TMEV v4.

## 4.5 | Functional enrichment analysis

For functional enrichment analysis, the DEGs obtained from the DESeq. 2 analysis were further analyzed using the ClusterProfiler package. ClusterProfiler provides various methods to perform functional enrichment analysis, including GO terms, Hallmarks of Cancer, and Cell Marker. Enriched pathways and gene sets were identified using appropriate statistical tests, and the results were visualized using dot plots and other visualization tools provided by ClusterProfiler.

## 4.6 | Kaposi's sarcoma gene expression signature profile

Kaposi's sarcoma KSHV and host RNA-seq profiles were retrieved from a previous study's GEO database GSE147704[21] and integrated with hMSC-derived samples for further analysis. We applied Pearson correlation with a complete linkage method for unsupervised clustering analysis.

## 4.7 | Human cytokine and angiogenic array

R&D Systems' Proteome Profiler Human XL Cytokine Array Kit (Catalog # ARY022B) and Proteome Profiler Human Angiogenesis Array Kit (Catalog # ARY007) were used to detect levels of 105 Cytokines and 55 different angiogenic-related proteins in MSC-KSHV$^{MEM}$ and MSC-KSHV$^{KS}$ cells after short- and long-term KSHV infection, respectively.

## 4.8 | Quantification of intracellular KSHV genomic DNA

To quantify intracellular KSHV DNA copy number, supernatants were removed, and cells were lyzed with trypsin ethylenediaminetetraacetic acid (Thermo Fisher Scientific). Trypsinization was halted with new media and centrifuged at 1000 rpm for 5 min. Pellets containing the cells were resuspended in 1× PBS to a final volume of 200 µL. We added 20 µL of proteinase K (QIAGEN protease) and followed the spin protocol per the manufacturer's instructions (DNA purification from blood or body fluids, QIAGEN; 51104). Intracellular viral DNA was calculated by quantitative PCR using the KSHV LANA gene and the cellular GAPDH gene as a reference for normalization. The relative KSHV copy number was expressed as a ratio of the copy number of the KSHV genome to the GAPDH DNA. LANA Primer Sequences: Forward: 5′- GCC TAT ACC AGG AAG TCC CA −3′; Reverse: 5′- GAG CCA CCG GTA AAG TAG GA −3′. GAPDH Primer Sequences: Forward: 5′- TCC CTG AGC TGA ACG GGA AG −3′; Reverse: 5′- GGA GGA GTG GGT GTC GCT GT −3′.

## 4.9 | Western blot analysis (WB)

Radioimmunoprecipitation assay lysis buffer (ThermoScientific) containing protease and phosphatase inhibitors (Sigma) was used to obtain protein lysates. 20 µg of protein was loaded and resolved in sodium dodecyl-sulfate polyacrylamide gel electrophoresis gel (Bio-Rad). The gel was transferred to a polyvinylidene fluoride membrane (Bio-Rad) and blocked with 5% bovine serum albumin (BSA) (Sigma) for 1 h to reduce nonspecific binding. Membranes were incubated with primary antibodies diluted in 5% BSA overnight. Protein bands were visualized using SuperSignal West Pico PLUS Chemiluminescent Substrate (ThermoScientific). We used the following antibodies: PDGFRa (sc398206, Santa Cruz), PECAM-1 (AF806, R&D system), CyclinD1 (sc718, Santa Cruz), Phos-AKT (Ab18206-100, Abcam), Akt (Pan)(Ab10660-100, Abcam), and Actin (4970T, Cell signaling).

## 4.10 | Statistical analysis

The statistical significance of the data was determined using a two-tailed Student's *t* test and two-way analysis of variance for multiple comparisons. A *p* value lower than 0.05 was considered significant. Statistical analysis was performed using GraphPad Prism 7. All values were expressed as means ± standard deviation.

## AUTHOR CONTRIBUTIONS

**Ezequiel Lacunza**: Conceptualization; data curation; formal analysis; methodology; validation; investigation; writing—original draft; and editing. **Anuj Ahuja**: Data curation; formal analysis; methodology; validation; investigation. **Martin Abba**: Data curation; formal analysis; methodology; validation; investigation; supervision; funding acquisition; project administration. **Omar A. Coso**: Investigation; supervision; funding acquisition; project administration. **Juan Carlos Ramos**: Investigation; supervision; funding acquisition; project administration; **Ethel Cesarman**: Supervision; editing. **Enrique A. Mesri**: Conceptualization; methodology; investigation; funding acquisition; project administration. **Julian Naipauer**: Conceptualization; data curation; formal analysis; methodology; validation; visualization; investigation; writing—original draft; editing; supervision; and funding acquisition.

## ACKNOWLEDGMENTS

The Oncogenomics Core Facility at the Sylvester Comprehensive Cancer Center from the University of Miami for performing high-throughput sequencing. J. N. was supported by the Miami CFAR Pilot grant P30AI073961. E. L., O. A. C., M. A., J. C. R., E. A. M., and J. N. were supported by the National Institutes of Health (NIH) grant U54CA221208. E. A. M. and J. C. R. were supported by the National Cancer Institute of the National Institutes of Healthc under Award Number P30CA240139. The content is solely the responsibility of the authors and does not necessarily represent the official views of the National Institutes of Health. A. A., E. A. M., and J. N. were supported by the NIH grant CA136387. Dr. Enrique A. Mesri, an inspiring scientist, a great mentor, and a friend, sadly passed away before sending the manuscript. For his dedication and contributions to the KSHV and viral oncology field, we will be always in debt to him.

## CONFLICT OF INTEREST STATEMENT

The authors declare no conflict of interest.

## DATA AVAILABILITY STATEMENT

The data that support the findings of this study are openly available in GEO: accession number GSE260925.

## ORCID

*Anuj Ahuja* http://orcid.org/0000-0002-0558-1356
*Julian Naipauer* http://orcid.org/0000-0001-6842-6815

## REFERENCES

1. Chang Y, Cesarman E, Pessin MS, et al. Identification of herpesvirus-like DNA sequences in AIDS-associated Kaposi's sarcoma. *Science*. 1994;266:1865-1869.
2. Ensoli B. Kaposi's sarcoma: a result of the interplay among inflammatory cytokines, angiogenic factors and viral agents. *Cytokine Growth Factor Rev*. 1998;9:63-83.
3. Ramos JC, Sin SH, Staudt MR, et al. Nuclear factor kappa B pathway associated biomarkers in AIDS defining malignancies. *Int J Cancer*. 2012;130:2728-2733. doi:10.1002/ijc.26302
4. Stürzl M, Brandstetter H, Zietz C, et al. Identification of interleukin-1 and platelet-derived growth factor-B as major mitogens for the spindle cells of Kaposi's sarcoma: a combined in vitro and in vivo analysis. *Oncogene*. 1995;10:2007-2016.
5. Mesri EA, Cesarman E, Boshoff C. Kaposi's sarcoma and its associated herpesvirus. *Nat Rev Cancer*. 2010;10:707-719. doi:10.1038/nrc2888
6. Mutlu AD, Cavallin LE, Vincent L, et al. In vivo-restricted and reversible malignancy induced by human herpesvirus-8 KSHV: a cell and animal model of virally induced Kaposi's sarcoma. *Cancer Cell*. 2007;11:245-258. doi:10.1016/j.ccr.2007.01.015
7. Jones T, Ye F, Bedolla R, et al. Direct and efficient cellular transformation of primary rat mesenchymal precursor cells by KSHV. *J Clin Invest*. 2012;122:1076-1081. doi:10.1172/JCI58530
8. Lee MS, Yuan H, Jeon H, et al. Human mesenchymal stem cells of diverse origins support persistent infection with Kaposi's sarcoma-associated herpesvirus and manifest distinct angiogenic, invasive, and transforming phenotypes. *mBio*. 2016;7:e02109-e02115. doi:10.1128/mBio.02109-15
9. Li Y, Zhong C, Liu D, et al. Evidence for Kaposi sarcoma originating from mesenchymal stem cell through KSHV-induced mesenchymal-to-endothelial transition. *Cancer Res*. 2018;78:230-245. doi:10.1158/0008-5472.CAN-17-1961
10. Parsons CH, Szomju B, Kedes DH. Susceptibility of human fetal mesencyhmal stem cells to Kaposi sarcoma-associated herpesvirus. *Blood*. 2004;104:2736-2738. doi:10.1182/blood-2004-02-0693
11. Yoo S, Jang J, Yoo C, Lee MS. Kaposi's sarcoma-associated herpesvirus infection of human bone-marrow-derived mesenchymal stem cells and their angiogenic potential. *Arch Virol*. 2014;159:2377-2386. doi:10.1007/s00705-014-2094-3
12. Gurzu S, Ciortea D, Munteanu T, Kezdi-Zaharia I, Jung I. Mesenchymal-to-endothelial transition in Kaposi sarcoma: a histo-genetic hypothesis based on a case series and literature review. *PLoS One*. 2013;8:e71530. doi:10.1371/journal.pone.0071530
13. Wang X, Chen W, Yuan Y. KSHV enhances mesenchymal stem cell homing and promotes KS-like pathogenesis. *Virology*. 2020;549:5-12. doi:10.1016/j.virol.2020.07.012
14. Chen W, Ding Y, Liu D, Lu Z, Wang Y, Yuan Y. Kaposi's sarcoma-associated herpesvirus vFLIP promotes MEndT to generate hybrid M/E state for tumorigenesis. *PLoS Pathog*. 2021;17:e1009600. doi:10.1371/journal.ppat.1009600
15. Naipauer J, Rosario S, Gupta S, et al. PDGFRA defines the mesenchymal stem cell Kaposi's sarcoma progenitors by enabling KSHV oncogenesis in an angiogenic environment. *PLoS Pathog*. 2019;15:e1008221. doi:10.1371/journal.ppat.1008221
16. Naipauer J, Mesri EA. The Kaposi's sarcoma progenitor enigma: KSHV-induced MEndT-EndMT axis. *Trends Mol Med*. 2023;29(3):188-200. doi:10.1016/j.molmed.2022.12.003
17. Vieira J, O'Hearn PM. Use of the red fluorescent protein as a marker of Kaposi's sarcoma-associated herpesvirus lytic gene expression. *Virology*. 2004;325:225-240. doi:10.1016/j.virol.2004.03.049
18. Burgess WH, Mehlman T, Marshak DR, Fraser BA, Maciag T. Structural evidence that endothelial cell growth factor beta is the precursor of both endothelial cell growth factor alpha and acidic fibroblast growth factor. *Proc Natl Acad Sci USA*. 1986;83:7216-7220. doi:10.1073/pnas.83.19.7216
19. Maciag T, Hoover GA, Weinstein R. High and low molecular weight forms of endothelial cell growth factor. *J Biol Chem*. 1982;257:5333-5336.
20. Tso FY, Kossenkov AV, Lidenge SJ, et al. RNA-Seq of Kaposi's sarcoma reveals alterations in glucose and lipid metabolism. *PLoS Pathog*. 2018;14:e1006844. doi:10.1371/journal.ppat.1006844
21. Lidenge SJ, Kossenkov AV, Tso FY, et al. Comparative transcriptome analysis of endemic and epidemic Kaposi's sarcoma (KS) lesions and the secondary role of HIV-1 in KS pathogenesis. *PLoS Pathog*. 2020;16:e1008681. doi:10.1371/journal.ppat.1008681
22. Casper C. The increasing burden of HIV-associated malignancies in resource-limited regions. *Annu Rev Med*. 2011;62:157-170. doi:10.1146/annurev-med-050409-103711
23. Cesarman E, Damania B, Krown SE, Martin J, Bower M, Whitby D. Kaposi sarcoma. *Nat Rev Dis Primers*. 2019;5:9. doi:10.1038/s41572-019-0060-9
24. Sullivan RJ, Pantanowitz L, Casper C, Stebbing J, Dezube BJ. HIV/AIDS: epidemiology, pathophysiology, and treatment of Kaposi sarcoma-associated herpesvirus disease: Kaposi sarcoma, primary effusion lymphoma, and multicentric Castleman disease. *Clin Infect Dis*. 2008;47:1209-1215. doi:10.1086/592298
25. Nguyen HQ, Magaret AS, Kitahata MM, Van Rompaey SE, Wald A, Casper C. Persistent Kaposi sarcoma in the era of highly active antiretroviral therapy: characterizing the predictors of clinical response. *AIDS*. 2008;22:937-945. doi:10.1097/QAD.0b013e3282ff6275
26. Thornton SC, Mueller SN, Levine EM. Human endothelial cells: use of heparin in cloning and long-term serial cultivation. *Science*. 1983;222:623-625. doi:10.1126/science.6635659

27. Ensoli B, Gendelman R, Markham P, et al. Synergy between basic fibroblast growth factor and HIV-1 Tat protein in induction of Kaposi's sarcoma. *Nature*. 1994;371:674-680. doi:10.1038/371674a0
28. Samaniego F, Markham PD, Gallo RC, Ensoli B. Inflammatory cytokines induce AIDS-Kaposi's sarcoma-derived spindle cells to produce and release basic fibroblast growth factor and enhance Kaposi's sarcoma-like lesion formation in nude mice. *J Immunol*. 1995;154:3582-3592.
29. Ensoli B, Nakamura S, Salahuddin SZ, et al. AIDS-Kaposi's sarcoma-derived cells express cytokines with autocrine and paracrine growth effects. *Science*. 1989;243:223-226.
30. Masiá M, Robledano C, Ortiz de la Tabla V, et al. Coinfection with human herpesvirus 8 is associated with persistent inflammation and immune activation in virologically suppressed HIV-infected patients. *PLoS One*. 2014;9:e105442. doi:10.1371/journal.pone.0105442
31. Pantanowitz L, Otis CN, Dezube BJ. Immunohistochemistry in Kaposi's sarcoma. *Clin Exp Dermatol*. 2010;35:68-72. doi:10.1111/j.1365-2230.2009.03707.x
32. Uccini S, Scarpino S, Ballarini F, et al. In situ study of chemokine and chemokine-receptor expression in Kaposi sarcoma. *Am J Dermatopathol*. 2003;25:377-383. doi:10.1097/00000372-200310000-00003
33. Ashlock BM, Ma Q, Issac B, Mesri EA. Productively infected murine Kaposi's sarcoma-like tumors define new animal models for studying and targeting KSHV oncogenesis and replication. *PLoS One*. 2014;9:e87324. doi:10.1371/journal.pone.0087324
34. Gomes SA, Rangel EB, Premer C, et al. S-nitrosoglutathione reductase (GSNOR) enhances vasculogenesis by mesenchymal stem cells. *Proc Natl Acad Sci USA*. 2013;110:2834-2839. doi:10.1073/pnas.1220185110
35. Myoung J, Ganem D. Generation of a doxycycline-inducible KSHV producer cell line of endothelial origin: maintenance of tight latency with efficient reactivation upon induction. *J Virol Methods*. 2011;174:12-21. doi:10.1016/j.jviromet.2011.03.012
36. Arias C, Weisburd B, Stern-Ginossar N, et al. KSHV 2.0: a comprehensive annotation of the Kaposi's sarcoma-associated herpesvirus genome using next-generation sequencing reveals novel genomic and functional features. *PLoS Pathog*. 2014;10:e1003847. doi:10.1371/journal.ppat.1003847

## SUPPORTING INFORMATION

Additional supporting information can be found online in the Supporting Information section at the end of this article.

**How to cite this article:** Lacunza E, Ahuja A, Coso OA, et al. Unveiling the role of KSHV-infected human mesenchymal stem cells in Kaposi's sarcoma initiation. *J Med Virol*. 2024;96:e29684. doi:10.1002/jmv.29684